



ÉCOLE
POLYTECHNIQUE
DE BRUXELLES

UNIVERSITÉ LIBRE DE BRUXELLES

Towards the predictive FE analysis of a metal/composite booster casing's thermomechanical integrity

Thèse présentée par Adélie CAPRON

en vue de l'obtention du grade académique de docteure en
Sciences de l'Ingénieur et Technologie

Année académique 2020-2021

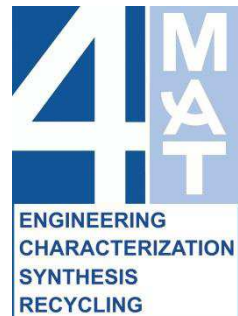
Sous la direction du Professeur Stéphane GODET,
promoteur

et du Professeur Thierry J. MASSART,
co-promoteur





Université libre de Bruxelles
École polytechnique de Bruxelles
Département 4MAT



Towards the predictive FE analysis of a metal/composite booster casing's thermomechanical integrity

Adélie Capron

Composition du jury:

Prof. Stéphane Godet (Promoteur)	Université libre de Bruxelles
Prof. Thierry J. Massart (Co-promoteur)	Université libre de Bruxelles
Prof. Marie-Paule Delplancke (Présidente)	Université libre de Bruxelles
Prof. Peter Berke (Secrétaire)	Université libre de Bruxelles
Prof. Thomas Pardoen	Université catholique de Louvain
Prof. Danny Van Hemelrijck	Vrije Universiteit Brussel
Dr. Ir. Johann Pancrace	Safran Aero Boosters

Bruxelles, le 30 novembre 2020

Abstract

In response to serious environmental and economic concerns, the design and production of aircrafts have been changing profoundly over the past decades with the nose-to-tail switch from metallic materials to lightweight composite materials such as carbon fibre reinforced plastic (CFRP). In this context, the present doctoral research work aimed to contribute to the development of a CFRP booster casing, a real innovation in the field initiated and conducted by Safran Aero Boosters. More specifically, this thesis addresses the matter of joining metal/CFRP hybrid structures, which are prone to possibly detrimental residual stresses.

The issue is treated with an approach combining experimental characterisation and finite element (FE) simulations. The multi-layered system's state of damage was systematically examined on hundreds of micrographs, and the outcome of this study is presented under the form of a statistical analysis. Further, the defects' 3D morphology is investigated by incremental polishing. A number of thermal and mechanical properties are measured by diverse physical tests on part of the constituent materials, i.e. the aerospace grade RTM6 epoxy resin, the structural Redux 322 epoxy film adhesive, and AISI 316L stainless steel. They are used as input data in a FE model of the multi-layer that is developed and progressively refined to obtain detailed residual stress fields after thermal loading. These results are compared to experimental data acquired by X-ray diffraction stress analysis and with the curvature-based Stoney formula. Cohesive elements are placed at specific locations within the FE model to allow simulating progressive damage. Peel tests,

mode I, mode II and mixed mode I/II fracture tests are thus performed in view of measuring the joint toughness. The results of these tests are discussed and the presence of residual stress in the fracture specimens is highlighted. Key information for the calibration of the cohesive law is finally identified via inverse FE analysis of the mode I test, this being a significant step in the process of building a damage predictive FE model of the multi-layered system.

Contents

1.	Introduction.....	25
1.1	General context	25
1.2	A composite low-pressure compressor at Safran Aero Boosters	29
1.3	Close-up on the composite casing.....	30
1.3.1	Design characteristics	31
1.3.2	Manufacturing process	35
1.3.3	Constituent materials	39
1.3.4	A damaged end product.....	48
1.4	Motivation, objective and outline of the thesis.....	50
2.	Scientific background	53
2.1	Introduction.....	53
2.2	About residual stress.....	53
2.2.1	Origin of residual stresses in multilayers	53
2.2.2	Analytical method for the evaluation of thermally induced residual stresses in multilayers	57
2.3	Fracture mechanics of multilayers	61
2.3.1	Introduction.....	61
2.3.2	Small-scale yielding	62
2.3.3	Stress intensity factor.....	63
2.3.4	Strain energy release rate	65
2.3.5	Relationship between G and K	67
2.3.6	Fracture toughness	68

2.3.7	Mixed mode fracture.....	70
2.4	Fracture toughness testing of adhesively bonded joints.....	75
2.4.1	Introduction.....	75
2.4.2	Beam-bending LEFM tests.....	77
2.4.3	Peel tests	87
2.5	Simulation of progressive damage with cohesive finite elements	91
2.5.1	Introduction.....	91
2.5.2	Cohesive zone and cohesive zone models.....	92
2.5.3	Definition of a cohesive zone length and implication	94
2.5.4	Approaches for modelling with cohesive elements	95
2.5.5	Description of the CZM used in this work	97
3.	Experimental investigation of the multilayer's damage state.....	101
3.1	Introduction.....	101
3.2	Damaged zones and types of damage.....	102
3.3	Statistical analysis of the multilayer's damage state	107
3.3.1	Methodology.....	107
3.3.2	Statistical analysis	109
3.3.3	Global review	118
3.4	Investigation of the 3D configuration and damage morphology at the inter-segments gap.....	120
3.5	Conclusion.....	128
4.	Thermo-mechanical characterisation of the constituent materials	129
4.1	Introduction.....	129
4.2	Effective properties of the CFRP composite laminate.....	130
4.2.1	Thermoelastic properties of the constituent laminae	131

4.2.2	Effective thermoelastic properties of the laminate	132
4.3	Properties of the RTM6 resin and the Redux 322 structural film adhesive.....	134
4.3.1	Materials	134
4.3.2	Thermal stability.....	136
4.3.3	Glass transition temperature.....	137
4.3.4	Mechanical and thermal properties.....	143
4.4	Properties of the as-rolled and micro-perforated 316L SS strips	155
4.4.1	Materials	156
4.4.2	Mechanical and thermal properties.....	156
4.5	Conclusion.....	168
5.	Evaluation of the thermally induced residual stresses in the multilayer.....	173
5.1	Introduction.....	173
5.2	Experimental evaluation of the residual stress state	174
5.2.1	X-ray stress analysis of free-standing and co-cured 316L SS strips	174
5.2.2	Curvature-based experimental evaluation of the residual stress with an extension of the Stoney formula.....	184
5.2.3	Conclusion.....	189
5.3	Analytical prediction of the through-thickness profile of thermally induced residual stress	189
5.3.1	Introduction.....	189
5.3.2	Through-thickness residual stress profiles thermally induced in the three-layered systems	189
5.4	FE prediction of the thermally induced residual stresses	192
5.4.1	Basic prediction of the residual stresses with model A	192
5.4.2	Refined prediction of the residual stress fields with model B..	197

5.5 Conclusion.....	220
6. Measurement of the critical SERRs of the co-cured joint	222
6.1 Introduction.....	222
6.2 Materials	223
6.2.1 Peel test specimens	223
6.2.2 Beam-type LEFM tests specimens	226
6.3 Adhesive fracture energy of the co-cured bond measured with the Fixed Arm Peel test	229
6.4 Mode I critical SERR of the co-cured joint measured with the Double Cantilever Beam test	241
6.4.1 Experimental procedure	242
6.4.2 Load-displacement curves and fracture surfaces.....	244
6.4.3 Curvature of the DCB specimen	251
6.4.4 Data reduction schemes.....	252
6.4.5 R-curves and mode I critical SERRs	255
6.4.6 G_{Ic} compared to G_A	257
6.5 Mode II and mixed mode I/II critical SERR of the co-cured joint measured with the End-Loaded Split test and the Fixed Ratio Mixed Mode test	257
6.5.1 Experimental procedures	258
6.5.2 Load-displacement curves.....	260
6.5.3 R-curves.....	260
6.5.4 Mode II and mixed mode I/II critical SERRs	264
6.6 Conclusion.....	265
7. Identification of the mode I cohesive law parameters by inverse FE analysis of the DCB test.....	269

7.1	Introduction.....	269
7.2	Presentation of the FE models	271
7.2.1	2D and 3D geometries.....	272
7.2.2	Mesh.....	272
7.2.3	Materials	274
7.2.4	Loads and boundary conditions.....	276
7.3	Parametric study and inverse analysis of the DCB test.....	279
7.3.1	Influence and selection of the penalty stiffness value	279
7.3.2	Influence of the spatial discretisation of the cohesive zone and selection of a criterion for mesh convergence.....	282
7.3.3	Identification of a value for the mode I critical SERR	285
7.3.4	Identification of a value for the mode I peak stress.....	287
7.4	Validation of the 2D approach with the 3D model.....	289
7.5	Preliminary identification of the fracture envelope and the mode coupling coefficient.....	291
7.6	Conclusion.....	293
8.	Conclusion and perspectives.....	295
8.1	Conclusion.....	295
8.2	Perspectives	299
A.	Dundurs' parameters	303
B.	Kinking, penetration, and deflection of an interface crack	304
B.1	Crack kinking.....	304
B.2	Crack penetration/deflection.....	305

C. Derivation of the analytical expression of G_{II} for the ELS test	306
D. Derivation of the analytical expression of $G_{I/II}$ for the FRMM test	307
E. Derivation of the analytical expression of Gdb , the total energy dissipated in bending of the peel arm	308
F. Classical Lamination Theory for the prediction of the effective thermoelastic properties of laminated media	310
F.1 Introduction.....	310
F.2 Model by Gudmundson and Zang.....	312
F.2.1 Constitutive relation of the lamina	313
F.2.2 Transformation from the lamina (principal) to the laminate (global) coordinate system	315
F.2.3 Constitutive relation of the laminate	316
G. Experimental methods.....	321
G.1 Thermogravimetric Analysis	321
G.2 Thermomechanical Analysis	322
G.2.1 Thermomechanical analysis of RTM6 and Redux 322.....	324
G.2.2 Thermomechanical analysis of the as-rolled AISI 316L SS strip....	325
.....	
G.3.1 Dynamic Mechanical Analysis of RTM6 and Redux 322.....	327
G.4 Quasi-static macroscopic tensile testing	329
G.4.1 Quasi-static macroscopic tensile testing of RTM6 and Redux 322.....	330

G.4.2	Quasi-static macroscopic tensile testing of as-rolled and micro-perforated AISI 316L SS	331
G.5	Resonant-based identification of elastic constants	335
G.5.1	Resonant-based identification of as-rolled and micro-perforated AISI 316L SS elastic constants	338
H.	Global analysis of the TMA curves.....	340
I.	Comment on the DMA curves.....	342
J.	Polynomial fits and discrete values of E-modulus and CTE.....	343
K.	X-ray stress analysis	346
K.1	Introduction.....	346
K.2	Fundamental principles of X-ray diffraction	346
K.3	XRD applied to stress analysis.....	349
K.3.1	Why stress can be quantified.....	349
K.3.2	How stress is quantified.....	353
K.3.3	Measurement procedure	359
L.	Bi-linear fit parameters of the steel strips' nominal tensile curves	363